European Journal of Mechanics A/Solids 49 (2015) 214–226

Contents lists available at ScienceDirect

European Journal of Mechanics A/Solids

journal homepage: www.elsevier.com/locate/ejmsol

Three-dimensional thermal stress analysis of laminated composite plates with general layups by a sampling surfaces method

G.M. Kulikov*, S.V. Plotnikova

Department of Applied Mathematics and Mechanics, Tambov State Technical University, Sovetskaya Street 106, Tambov 392000, Russia

ARTICLE INFO

Article history:
Received 31 March 2013
Accepted 28 July 2014
Available online 7 August 2014

Keywords:
3D thermal stress analysis
Angle-ply laminates
Sampling surfaces method

ABSTRACT

A paper focuses on the application of the method of sampling surfaces (SaS) to three-dimensional (3D) steady-state thermoelasticity problems for orthotropic and anisotropic laminated plates subjected to thermal loading. This method is based on selecting inside the nth layer I_n not equally spaced SaS parallel to the middle surface of the plate in order to choose temperatures and displacements of these surfaces as basic plate variables. Such an idea permits the presentation of the proposed thermoelastic laminated plate formulation in a very compact form. It is worth noting that the SaS are located inside each layer at Chebyshev polynomial nodes that leads to a uniform convergence of the SaS method. As a result, the SaS method can be applied efficiently to the 3D stress analysis of cross-ply and angle-ply composite plates with a specified accuracy utilizing the sufficient number of SaS.

1. Introduction

Three-dimensional (3D) exact analysis of laminated composite plates has attracted the considerable attention during past forty years. This is due to the fact that the validity of approximate plate theories and plate finite elements can be assessed by comparing their predictions with 3D exact solutions. The analytical solution of elasticity for a simply supported isotropic rectangular plate was presented by Vlasov (1957). The extensions of Vlasov's solution to orthotropic laminated plates were done by Pagano (1969, 1970a), and Srinivas and Rao (1970). Murakami (1993) generalized the work of Pagano (1969) to the cylindrical bending of simply supported laminates subjected to thermal loading. Tungikar and Rao (1994), Noor et al. (1994) and Bhaskar et al. (1996)) derived 3D exact solutions for laminated cross-ply rectangular plates subjected to thermomechanical loads. Tauchert (1980) gave 3D exact solutions of thermoelasticity for simply supported orthotropic laminates using the method of displacement potentials. The analytical solutions for functionally graded single-layer and laminated plates under mechanical and thermal loads were derived by Cheng and Batra (2000), Reddy and Cheng (2001), Vel and Batra (2002), Kashtalyan (2004), and Woodward and Kashtalyan (2011).

Pagano (1970b) presented the exact solution for the cylindrical bending of laminated composite plates with general layups. The response of a thermoelastic anisotropic laminated plate in cylindrical bending was investigated analytically by Bhaskar et al. (1996), and Vel and Batra (2001). The developments for antisymmetric angle-ply laminates in the framework of the 3D theory were carried out by Noor and Burton (1990), Savoia and Reddy (1992, 1995), and Kulikov and Plotnikova (2012a). However, the reliable 3D solutions for thermoelastic laminated composite plates of general lay-up configurations can not be found in the current literature. Partially, the present paper serves to fill the gap of knowledge in this research area.

To solve such a problem, we invoke the efficient method of sampling surfaces (SaS) developed recently by Kulikov and Plotnikova (2012a, 2012b, 2013, 2014) for the analysis of orthotropic and anisotropic laminated plates and shells. As SaS denoted here by $\Omega^{(n)1}, \Omega^{(n)2}, \ldots, \Omega^{(n)I_n}$, we choose outer surfaces and any inner surfaces inside the nth layer of the plate and introduce temperatures $T^{(n)1}, T^{(n)2}, \ldots, T^{(n)I_n}$ and displacement vectors $\mathbf{u}^{(n)1}, \mathbf{u}^{(n)2}, \ldots, \mathbf{u}^{(n)I_n}$ of these surfaces as basic plate variables, where I_n is the total number of SaS chosen for each layer ($I_n \geq 3$). Such choice of temperatures and displacements with the consequent use of Lagrange polynomials of degree $I_n - 1$ in the thickness direction for each layer permits the presentation of governing equations of the thermal laminated plate formulation in a very compact form. It is necessary to note that the term SaS should not be confused with such terms as fictitious interfaces or mathematical interfaces, which are extensively used in layer-wise theories. The main difference consists in the lack of possibility to employ polynomials of high degree in the thickness direction because in conventional layer-wise thermal shell theories only third and fourth order polynomial interpolations are admissible

* Corresponding author.
E-mail addresses: gmkulikov@mail.ru, kulikov@apmath.tstu.ru (G.M. Kulikov).

http://dx.doi.org/10.1016/j.euromechsol.2014.07.011
0997-7538/

(see, e.g. Carrera, 2000, 2005; Carrera and Ciuffreda, 2004; Robaldo et al., 2005; Robaldo and Carrera, 2007). This restricts the use of the fictitious/mathematical interfaces technique for the 3D thermal stress analysis of thick laminated composite plates. On the contrary, the SaS method allows the use of Lagrange polynomials of *high* degree. This fact gives the opportunity to derive the 3D solutions for laminated composite plates with a prescribed accuracy employing a sufficiently large number of not equally spaced SaS.

It is worth noting that the developed approach with the arbitrary number of equally spaced SaS (Kulikov and Plotnikova, 2011) does not work properly with the Lagrange polynomials of high degree because the Runge's phenomenon can occur, which yields the wild oscillation at the edges of the interval when the user deals with any specific functions. If the number of equally spaced nodes is increased then the oscillations become even larger. However, the use of Chebyshev polynomial nodes (Burden and Faires, 2010) inside each layer can help to improve significantly the behavior of the Lagrange polynomials of high degree because such a choice allows one to minimize uniformly the error due to Lagrange interpolation.

The origins of using the SaS can be found in contributions of Kulikov (2001) and Kulikov and Carrera (2008) in which three, four and five equally spaced SaS are employed. The SaS method with the arbitrary number of equispaced SaS is considered by Kulikov and Plotnikova (2011). The more general approach with the SaS located at Chebyshev polynomial nodes has been developed later (Kulikov and Plotnikova, 2012a, 2012b).

2. Description of temperature field

Consider a laminated plate of the thickness h. Let the middle surface Ω be described by Cartesian coordinates x_1 and x_2. The coordinate x_3 is oriented in the thickness direction. The transverse coordinates of SaS inside the nth layer are defined as

$$\begin{aligned} &x_3^{(n)1} = x_3^{[n-1]}, \quad x_3^{(n)I_n} = x_3^{[n]}, \\ &x_3^{(n)m_n} = \frac{1}{2}\left(x_3^{[n-1]} + x_3^{[n]}\right) - \frac{1}{2}h_n \cos\left(\pi \frac{2m_n - 3}{2(I_n - 2)}\right), \end{aligned} \tag{1}$$

where $x_3^{[n-1]}$ and $x_3^{[n]}$ are the transverse coordinates of layer interfaces $\Omega^{[n-1]}$ and $\Omega^{[n]}$ (Fig. 1); $h_n = x_3^{[n]} - x_3^{[n-1]}$ is the thickness of the nth layer; I_n is the number of SaS corresponding to the nth layer; the index n identifies the belonging of any quantity to the nth layer and runs from 1 to N; N is the total number of layers; the index m_n identifies the belonging of any quantity to the inner SaS of the nth layer and runs from 2 to $I_n - 1$, whereas the indices i_n, j_n, k_n to be introduced later for describing all SaS of the nth layer run from 1 to I_n. Besides, the tensorial indices i, j, k, l range from 1 to 3 and Greek indices α, β range from 1 to 2.

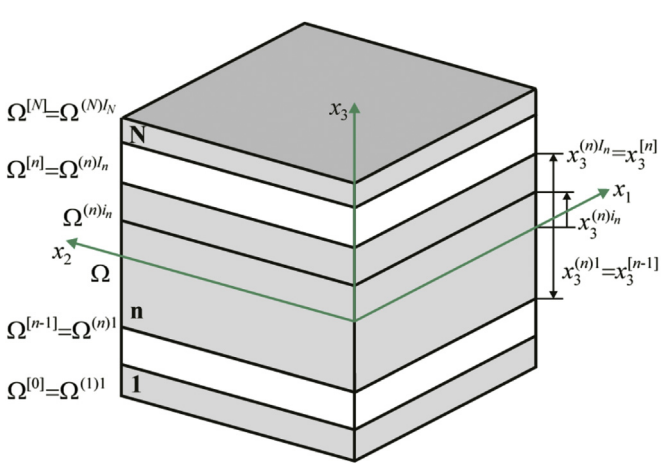

Fig. 1. Geometry of the laminated plate.

Remark 1. The transverse coordinates of inner SaS (1) coincide with the coordinates of Chebyshev polynomial nodes (Burden and Faires, 2010). This fact has a great meaning for a convergence of the SaS method (Kulikov and Plotnikova, 2012a, 2012b).

The relation between the temperature T and the temperature gradient $\mathbf{\Gamma}$ is given by

$$\mathbf{\Gamma} = \nabla T. \tag{2}$$

In a component form, it can be written as

$$\Gamma_i = T_{,i}, \tag{3}$$

where the symbol $(\ldots)_{,i}$ stands for the partial derivatives with respect to coordinates x_i.

We start now with the first fundamental assumption of the proposed thermoelastic laminated plate formulation. Let us assume that temperature and temperature gradient fields are distributed through the thickness of the nth layer as follows:

$$T^{(n)} = \sum_{i_n} L^{(n)i_n} T^{(n)i_n}, \quad x_3^{[n-1]} \le x_3 \le x_3^{[n]}, \tag{4}$$

$$\Gamma_i^{(n)} = \sum_{i_n} L^{(n)i_n} \Gamma_i^{(n)i_n}, \quad x_3^{[n-1]} \le x_3 \le x_3^{[n]}, \tag{5}$$

where $T^{(n)i_n}(x_1, x_2)$ are the temperatures of SaS of the nth layer $\Omega^{(n)i_n}$; $\Gamma_i^{(n)i_n}(x_1, x_2)$ are the components of the temperature gradient at the same SaS; $L^{(n)i_n}(x_3)$ are the Lagrange polynomials of degree $I_n - 1$ defined as

$$T^{(n)i_n} = T\left(x_3^{(n)i_n}\right), \tag{6}$$

$$\Gamma_i^{(n)i_n} = \Gamma_i\left(x_3^{(n)i_n}\right), \tag{7}$$

$$L^{(n)i_n} = \prod_{j_n \ne i_n} \frac{x_3 - x_3^{(n)j_n}}{x_3^{(n)i_n} - x_3^{(n)j_n}}. \tag{8}$$

The use of relations (3), (4), (6) and (7) yields

$$\Gamma_\alpha^{(n)i_n} = T_{,\alpha}^{(n)i_n}, \tag{9}$$

$$\Gamma_3^{(n)i_n} = \sum_{j_n} M^{(n)j_n}\left(x_3^{(n)i_n}\right) T^{(n)j_n}, \tag{10}$$

where $M^{(n)j_n} = L_{,3}^{(n)j_n}$ are the derivatives of Lagrange polynomials, which are calculated at SaS as follows:

$$\begin{aligned} &M^{(n)j_n}\left(x_3^{(n)i_n}\right) = \frac{1}{x_3^{(n)j_n} - x_3^{(n)i_n}} \prod_{k_n \ne i_n, j_n} \frac{x_3^{(n)i_n} - x_3^{(n)k_n}}{x_3^{(n)j_n} - x_3^{(n)k_n}} \quad \text{for } j_n \ne i_n, \\ &M^{(n)i_n}\left(x_3^{(n)i_n}\right) = -\sum_{j_n \ne i_n} M^{(n)j_n}\left(x_3^{(n)i_n}\right). \end{aligned} \tag{11}$$

It is seen from Eq. (10) that the transverse component of the temperature gradient $\Gamma_3^{(n)i_n}$ is represented as a *linear combination* of temperatures of all SaS of the nth layer $T^{(n)j_n}$.

3. Description of displacement and strain fields

The strain tensor ε_{ij} is given by

$$2\varepsilon_{ij} = u_{i,j} + u_{j,i}, \tag{12}$$

where u_i are the displacements of the plate. In particular, the strain tensor at SaS of the nth layer $\varepsilon_{ij}^{(n)i_n}(x_1, x_2)$ can be expressed as

$$\begin{aligned} 2\varepsilon_{\alpha\beta}^{(n)i_n} &= 2\varepsilon_{\alpha\beta}\left(x_3^{(n)i_n}\right) = u_{\alpha,\beta}^{(n)i_n} + u_{\beta,\alpha}^{(n)i_n}, \\ 2\varepsilon_{\alpha3}^{(n)i_n} &= 2\varepsilon_{\alpha3}\left(x_3^{(n)i_n}\right) = \beta_\alpha^{(n)i_n} + u_{3,\alpha}^{(n)i_n}, \\ \varepsilon_{33}^{(n)i_n} &= \varepsilon_{33}\left(x_3^{(n)i_n}\right) = \beta_3^{(n)i_n}, \end{aligned} \tag{13}$$

where $u_i^{(n)i_n}(x_1, x_2)$ are the displacements of SaS of the nth layer $\Omega^{(n)i_n}$; $\beta_i^{(n)i_n}(x_1, x_2)$ are the derivatives of displacements with respect to the thickness coordinate at the same SaS defined as

$$u_i^{(n)i_n} = u_i\left(x_3^{(n)i_n}\right), \tag{14}$$

$$\beta_i^{(n)i_n} = u_{i,3}\left(x_3^{(n)i_n}\right). \tag{15}$$

The following step consists in a choice of the approximation of displacements and strains through the thickness of the nth layer. It is apparent that displacement and strain distributions should be chosen similar to the thermal distributions (4) and (5). Thus, the second fundamental assumption of the developed thermoelastic laminated plate formulation can be written as

$$u_i^{(n)} = \sum_{i_n} L^{(n)i_n} u_i^{(n)i_n}, \quad x_3^{[n-1]} \le x_3 \le x_3^{[n]}, \tag{16}$$

$$\varepsilon_{ij}^{(n)} = \sum_{i_n} L^{(n)i_n} \varepsilon_{ij}^{(n)i_n}, \quad x_3^{[n-1]} \le x_3 \le x_3^{[n]}. \tag{17}$$

The use of Eqs. (15) and (16) yields

$$\beta_i^{(n)i_n} = \sum_{j_n} M^{(n)j_n}\left(x_3^{(n)i_n}\right) u_i^{(n)j_n}, \tag{18}$$

which is similar to Eq. (10). So, the key functions $\beta_i^{(n)i_n}$ of the proposed plate formulation are represented as a *linear combination* of displacements of SaS of the nth layer $u_i^{(n)j_n}$.

4. Variational formulation of heat conduction problem

The variational equation for the laminated plate can be written as

$$\delta J = 0, \tag{19}$$

where J is the basic functional of the heat conduction theory given by

$$J = \frac{1}{2}\iint_\Omega \sum_n \int_{x_3^{[n-1]}}^{x_3^{[n]}} q_i^{(n)} \Gamma_i^{(n)} \mathrm{d}x_1 \mathrm{d}x_2 \mathrm{d}x_3 - \iint_{\overline{\Omega}} TQ_n \mathrm{d}\Omega, \tag{20}$$

where $q_i^{(n)}$ are the components of the heat flux vector of the nth layer; Q_n is the specified heat flux on the boundary surface $\overline{\Omega} = \Omega^{[0]} + \Omega^{[N]} + \Sigma$, where Σ is the edge boundary surface of the plate.

Substituting the through-thickness distribution (5) in Eq. (20) and introducing heat flux resultants

$$R_i^{(n)i_n} = \int_{x_3^{[n-1]}}^{x_3^{[n]}} q_i^{(n)} L^{(n)i_n} \mathrm{d}x_3, \tag{21}$$

one obtains

$$J = \frac{1}{2}\iint_\Omega \sum_n \sum_{i_n} R_i^{(n)i_n} \Gamma_i^{(n)i_n} \mathrm{d}x_1 \mathrm{d}x_2 - \iint_{\overline{\Omega}} TQ_n \mathrm{d}\Omega. \tag{22}$$

Now, we accept the third fundamental assumption of the proposed thermal laminated plate formulation. Let the constitutive equations be the Fourier's heat conduction equations:

$$q_i^{(n)} = -k_{ij}^{(n)} \Gamma_j^{(n)}, \quad x_3^{[n-1]} \le x_3 \le x_3^{[n]}, \tag{23}$$

where $k_{ij}^{(n)}$ are the components of the thermal conductivity tensor of the nth layer.

Inserting (23) in Eq. (21) and taking into account (5), we obtain

$$R_i^{(n)i_n} = -\sum_{j_n} \Lambda^{(n)i_n j_n} k_{ij}^{(n)} \Gamma_j^{(n)j_n}, \tag{24}$$

where

$$\Lambda^{(n)i_n j_n} = \int_{x_3^{[n-1]}}^{x_3^{[n]}} L^{(n)i_n} L^{(n)j_n} \mathrm{d}x_3. \tag{25}$$

5. Variational formulation of thermoelastic plate problem

The variational equation for the thermoelastic laminated plate in the case of conservative loading can be written as

$$\delta\Pi = 0, \tag{26}$$

where Π is the basic functional of the thermoelasticity theory given by

$$\Pi = \frac{1}{2}\iint_\Omega \sum_n \int_{x_3^{[n-1]}}^{x_3^{[n]}} \left(\sigma_{ij}^{(n)} \varepsilon_{ij}^{(n)} - \eta^{(n)} \Theta^{(n)}\right) \mathrm{d}x_1 \mathrm{d}x_2 \mathrm{d}x_3 - W, \tag{27}$$

$$W = \iint_\Omega \left(p_i^+ u_i^{[N]} - p_i^- u_i^{[0]}\right) \mathrm{d}x_1 \mathrm{d}x_2 + W_\Sigma, \tag{28}$$

where $\sigma_{ij}^{(n)}$ are the components of the stress tensor of the nth layer; $\eta^{(n)}$ is the entropy density of the nth layer; $u_i^{[0]} = u_i^{(1)1}$ and $u_i^{[N]} = u_i^{(N)I_N}$ are the displacements of bottom and top surfaces $\Omega^{[0]}$ and $\Omega^{[N]}$; p_i^- and p_i^+ are the loads acting on bottom and top surfaces; W_Σ is the work done by external thermomechanical loads applied to the edge surface Σ; $\Theta^{(n)}$ is the temperature rise from the initial reference temperature T_0 defined as

$$\Theta^{(n)} = T^{(n)} - T_0. \tag{29}$$

Substituting the strain distribution (17) and the temperature distribution

$$\Theta^{(n)} = \sum_{i_n} L^{(n)i_n} \Theta^{(n)i_n}, \quad x_3^{[n-1]} \le x_3 \le x_3^{[n]}, \tag{30}$$

which follows directly from Eqs. (4) and (29), in Eq. (27) and introducing stress resultants

$$H_{ij}^{(n)i_n} = \int_{x_3^{[n-1]}}^{x_3^{[n]}} \sigma_{ij}^{(n)} L^{(n)i_n} \mathrm{d}x_3 \tag{31}$$

and entropy resultants

$$S^{(n)i_n} = \int_{x_3^{[n-1]}}^{x_3^{[n]}} \eta^{(n)} L^{(n)i_n} \mathrm{d}x_3, \tag{32}$$

one obtains

$$\Pi = \frac{1}{2} \iint_{\Omega} \sum_n \sum_{i_n} \left(H_{ij}^{(n)i_n} \varepsilon_{ij}^{(n)i_n} - S^{(n)i_n} \Theta^{(n)i_n} \right) \mathrm{d}x_1 \mathrm{d}x_2 - W, \tag{33}$$

where $\Theta^{(n)i_n}(x_1, x_2)$ are the temperature rises of SaS of the nth layer $\Omega^{(n)i_n}$.

Finally, we introduce the fourth fundamental assumption of the proposed thermoelastic laminated plate formulation. Consider for simplicity the case of linear thermoelastic materials. Therefore, constitutive equations (Reddy, 2004) are written as follows:

$$\sigma_{ij}^{(n)} = C_{ijk\ell}^{(n)} \varepsilon_{k\ell}^{(n)} - \gamma_{ij}^{(n)} \Theta^{(n)}, \quad x_3^{[n-1]} \le x_3 \le x_3^{[n]}, \tag{34}$$

$$\eta^{(n)} = \gamma_{ij}^{(n)} \varepsilon_{ij}^{(n)} + \chi^{(n)} \Theta^{(n)}, \quad x_3^{[n-1]} \le x_3 \le x_3^{[n]}, \tag{35}$$

where $C_{ijkl}^{(n)}$ are the elastic constants of the nth layer; $\gamma_{ij}^{(n)}$ are the thermal stress coefficients of the nth layer; $\chi^{(n)}$ is the entropy–temperature coefficient defined as

$$\chi^{(n)} = \rho^{(n)} c_{\mathrm{v}}^{(n)} \Big/ T_0, \tag{36}$$

where $\rho^{(n)}$ and $c_{\mathrm{v}}^{(n)}$ are the mass density and the specific heat per unit mass of the nth layer at constant strain.

Substituting constitutive equations (34) and (35) correspondingly in Eqs. (31) and (32) and allowing for strain and temperature distributions (17) and (30), we have

$$H_{ij}^{(n)i_n} = \sum_{j_n} \Lambda^{(n)i_n j_n} \left(C_{ijk\ell}^{(n)} \varepsilon_{k\ell}^{(n)j_n} - \gamma_{ij}^{(n)} \Theta^{(n)j_n} \right), \tag{37}$$

$$S^{(n)i_n} = \sum_{j_n} \Lambda^{(n)i_n j_n} \left(\gamma_{ij}^{(n)} \varepsilon_{ij}^{(n)j_n} + \chi^{(n)} \Theta^{(n)j_n} \right). \tag{38}$$

In formulas (37) and (38), coefficients $\Lambda^{(n)i_n j_n}$ are calculated according to Eq. (25).

6. Analytical solution for laminated orthotropic plates

In this section, we study a laminated orthotropic rectangular plate subjected to thermomechanical loading. The boundary conditions for a simply supported plate with edges maintained at the reference temperature can be written as

$$\begin{aligned} &\sigma_{11}^{(n)} = u_2^{(n)} = u_3^{(n)} = \Theta^{(n)} = 0 \quad \text{at } x_1 = 0 \text{ and } x_1 = a, \\ &\sigma_{22}^{(n)} = u_1^{(n)} = u_3^{(n)} = \Theta^{(n)} = 0 \quad \text{at } x_2 = 0 \text{ and } x_2 = b, \end{aligned} \tag{39}$$

where a and b are the plate dimensions. To satisfy boundary conditions, we search for the analytical solution by a method of double Fourier series expansions

$$\Theta^{(n)i_n} = \sum_{r,s} \Theta_{rs}^{(n)i_n} \sin\frac{r\pi x_1}{a} \sin\frac{s\pi x_2}{b}, \tag{40}$$

$$\begin{aligned} u_1^{(n)i_n} &= \sum_{r,s} u_{1rs}^{(n)i_n} \cos\frac{r\pi x_1}{a} \sin\frac{s\pi x_2}{b}, \\ u_2^{(n)i_n} &= \sum_{r,s} u_{2rs}^{(n)i_n} \sin\frac{r\pi x_1}{a} \cos\frac{s\pi x_2}{b}, \\ u_3^{(n)i_n} &= \sum_{r,s} u_{3rs}^{(n)i_n} \sin\frac{r\pi x_1}{a} \sin\frac{s\pi x_2}{b}, \end{aligned} \tag{41}$$

where r and s are the wave numbers in plane directions. The external mechanical loads are also expanded in double Fourier series.

Substituting Fourier series (40) in Eqs. (9), (10), (22) and (24), and taking into account (29) and (30), one derives

$$J = \sum_{r,s} J_{rs} \left(\Theta_{rs}^{(n)i_n} \right). \tag{42}$$

Invoking the variational equations (19) and (42), we arrive at the system of linear algebraic equations

$$\frac{\partial J_{rs}}{\partial \Theta_{rs}^{(n)i_n}} = 0, \tag{43}$$

of order K, where $K = \sum_n I_n - N + 1$. Thus, temperature rises of SaS of the nth layer $\Theta_{rs}^{(n)i_n}$ can be found by using a method of Gaussian elimination.

Substituting next Fourier series (40) and (41), and Fourier series corresponding to mechanical loading in Eqs. (13), (18), (28), (33), (37) and (38), we obtain

$$\Pi = \sum_{r,s} \Pi_{rs} \left(u_{irs}^{(n)i_n}, \Theta_{rs}^{(n)i_n} \right). \tag{44}$$

The use of the variational equations (26) and (44) yields a system of linear algebraic equations

$$\frac{\partial \Pi_{rs}}{\partial u_{irs}^{(n)i_n}} = 0 \tag{45}$$

of order $3K$. The linear system (45) is solved again by a method of Gaussian elimination.

The described algorithm was performed with the Symbolic Math Toolbox, which incorporates symbolic computations into the numeric environment of MATLAB. This gives an opportunity to obtain analytical solutions for laminated orthotropic rectangular plates with a specified accuracy employing the sufficient number of SaS.

6.1. Single-layer square plate under mechanical loading

Consider a simply supported isotropic square plate subjected to transverse sinusoidal loading acting on its top surface

$$p_3^+ = p_0 \sin\frac{\pi x_1}{a} \sin\frac{\pi x_2}{b}, \quad p_3^- = 0, \tag{46}$$

where $p_0 = 1$ Pa.

Table 1
Results for a single-layer square plate with $a/h = 3$.

I_1	$-\bar{u}_1(0.5)$	$\bar{u}_3(0)$	$\bar{\sigma}_{11}(0.5)$	$-\bar{\sigma}_{12}(0.5)$	$\bar{\sigma}_{13}(0)$	$\bar{\sigma}_{33}(0)$
3	0.3986372494504680	1.278878243389591	1.999302146854837	0.8349039028805547	0.4977436151168003	0.4752837277628003
7	0.4358933937131948	1.342554953466513	2.124032428288413	0.9129329889584641	0.7022762666060094	0.4943950643281928
11	0.4358933942603120	1.342554689543095	2.124018410314048	0.9129329901043438	0.7023022083223538	0.4944039935419638
15	0.4358933942603121	1.342554689542491	2.124018410193782	0.9129329901043439	0.7023022084767580	0.4944039936052152
19	0.4358933942603120	1.342554689542491	2.124018410193780	0.9129329901043437	0.7023022084767578	0.4944039936052150
Exact[a]	0.4358933942603120	1.342554689542491	2.124018410193781	0.9129329901043437	0.7023022084767578	0.4944039936052149

[a] The exact results have been obtained by the authors using the closed-form solution of Vlasov (1957).

The geometrical and mechanical parameters of the plate are taken to be $a = b = 1$ m, $E = 10^7$ Pa and $\nu = 0.3$, where E is the Young modulus and ν is the Poisson ratio. To compare the results derived with the closed-form solution of elasticity (Vlasov, 1957), we introduce the following dimensionless variables at crucial points as functions of the z-coordinate:

$$\bar{u}_1 = Gu_1(0, a/2, z)/hp_0, \quad \bar{u}_3 = Gu_3(a/2, a/2, z)/hp_0,$$
$$\bar{\sigma}_{11} = \sigma_{11}(a/2, a/2, z)/p_0,$$

$$\bar{\sigma}_{12} = \sigma_{12}(0, 0, z)/p_0, \quad \bar{\sigma}_{13} = \sigma_{13}(0, a/2, z)/p_0,$$
$$\bar{\sigma}_{33} = \sigma_{33}(a/2, a/2, z)/p_0,$$

where G is the shear modulus.

Tables 1 and 2 show results of the convergence study due to increasing the number of SaS. As turned out, the SaS method provides 15 right digits for all basic variables utilizing 13 inner SaS inside the plate body. This implies that the SaS formulation permits the derivation of analytical solutions for plates, which asymptotically approach the 3D exact solutions of elasticity as the number of SaS $I_1 \to \infty$. It should be noted that herein the bottom and top surfaces are not included into a set of SaS because the use of only Chebyshev polynomial nodes allows one to minimize uniformly the error due to Lagrange interpolation. Fig. 2 displays distributions of transverse stresses through the thickness of the plate for different values of the slenderness ratio a/h and the number of SaS. It is seen that the use of conventional plate theories based on the quadratic polynomial interpolation of displacements in the thickness direction that corresponds to the choice of three SaS in a proposed SaS formulation ($I_1 = 3$) yields a poor prediction of through-thickness distributions of transverse stresses for thick and thin plates. Moreover, widespread cubic polynomial interpolations of the displacement field that corresponds to the case of four SaS ($I_1 = 4$) still incorrectly describe the through-thickness distribution of transverse normal stresses for thick and thin plates. The implementation of the numerical algorithm by means of three MATLAB modules is presented in Appendix.

6.2. Sandwich square plate under temperature loading

Next, we consider a sandwich square plate subjected to temperature loading applied to bottom and top surfaces

$$\Theta^{[0]} = \Theta_0 \sin\frac{\pi x_1}{a} \sin\frac{\pi x_2}{b}, \quad \Theta^{[N]} = -\Theta_0 \sin\frac{\pi x_1}{a} \sin\frac{\pi x_2}{b}, \tag{47}$$

where $\Theta_0 = 1$ K and $T_0 = 293$ K. The face sheets of the sandwich plate with ply thicknesses [0.2h/0.6h/0.2h] are composed of the graphite–epoxy composite orientated in x_1-direction with material properties: $E_L = 200$ GPa, $E_T = 8$ GPa, $G_{LT} = 5$ GPa, $G_{TT} = 2.2$ GPa, $\nu_{LT} = 0.25$, $\nu_{TT} = 0.35$, $\alpha_L = -2 \times 10^{-6}$ 1/K, $\alpha_T = 50 \times 10^{-6}$ 1/K, $k_L = 50$ W/mK, $k_T = 0.5$ W/mK, $\rho = 1800$ kg/m^3 and $c_v = 900$ J/kgK. The material properties of the core are chosen to be $E_1 = E_2 = 1$ GPa, $E_3 = 2$ GPa, $G_{12} = 0.37$ GPa, $G_{13} = G_{23} = 0.8$ GPa, $\nu_{12} = 0.35$, $\nu_{13} = \nu_{23} = 0.25$, $\alpha_{11} = \alpha_{22} = \alpha_{33} = 30 \times 10^{-6}$ 1/K, $k_{11} = k_{22} = k_{33} = 50$ W/mK, $\rho = 100$ kg/m^3 and $c_v = 900$ J/kgK. To compare the results with the 3D analytical solution (Savoia and Reddy, 1995), we take $a = b = 1$ m and introduce dimensionless variables at crucial points as functions of the z-coordinate

$$\bar{u}_1 = u_1(0, a/2, z)/a\alpha_r\Theta_0, \quad \bar{u}_2 = u_2(a/2, 0, z)/a\alpha_r\Theta_0,$$
$$\bar{u}_3 = u_3(a/2, a/2, z)/a\alpha_r\Theta_0,$$

$$\bar{\sigma}_{11} = \sigma_{11}(a/2, a/2, z)/E_r\alpha_r\Theta_0,$$
$$\bar{\sigma}_{22} = \sigma_{22}(a/2, a/2, z)/E_r\alpha_r\Theta_0, \quad \bar{\sigma}_{12} = \sigma_{12}(0, 0, z)/E_r\alpha_r\Theta_0,$$

$$\bar{\sigma}_{13} = \sigma_{13}(0, a/2, z)/E_r\alpha_r\Theta_0,$$
$$\sigma_{23} = \sigma_{23}(a/2, 0, z)/E_r\alpha_r\Theta_0, \quad \bar{\sigma}_{33} = \sigma_{33}(a/2, a/2, z)/E_r\alpha_r\Theta_0,$$

$$\bar{\Theta} = \Theta(a/2, a/2, z)/\Theta_0, \quad \bar{q}_3 = aq_3(a/2, a/2, z)/k_r\Theta_0,$$
$$\bar{\eta} = \eta(a/2, a/2, z)\Big/E_r\alpha_r^2\Theta_0,$$

where $E_r = 1$ GPa, $\alpha_r = 10^{-6}$ 1/K, $k_r = 1$ W/mK and $z = x_3/h$.

Tables 3 and 4 list the results of the convergence study utilizing a various number of SaS I_n inside the nth layer. These results demonstrate convincingly the high potential of the developed thermoelastic laminated plate formulation. It is important to note that here both outer surfaces and both interfaces are included into a set of SaS because of the use of boundary conditions (47). Fig. 3 displays through-thickness distributions of the temperature, heat flux, transverse stresses and entropy for different slenderness ratios a/h employing 11 SaS for each layer. A comparison with the

Table 2
Results for a single-layer square plate with $a/h = 10$.

I_1	$-\bar{u}_1(0.5)$	$\bar{u}_3(0)$	$\bar{\sigma}_{11}(0.5)$	$-\bar{\sigma}_{12}(0.5)$	$\bar{\sigma}_{13}(0)$	$\bar{\sigma}_{33}(0)$
3	16.69442044348862	112.4420178073405	19.91690124596434	10.48941372424062	1.706202131658078	0.4978329738513218
7	16.81014395019634	113.1720941024937	20.04394635519068	10.56212494794475	2.383373139214406	0.4999497585886086
11	16.81014395019644	113.1720941004914	20.04394633189751	10.56212494794481	2.383373791176881	0.4999497657893389
15	16.81014395019644	113.1720941004913	20.04394633189750	10.56212494794481	2.383373791176909	0.4999497657893389
19	16.81014395019645	113.1720941004914	20.04394633189751	10.56212494794481	2.383373791176910	0.4999497657893400
Exact[a]	16.81014395019644	113.1720941004914	20.04394633189751	10.56212494794481	2.383373791176911	0.4999497657893391

[a] The exact results have been obtained by the authors using the closed-form solution of Vlasov (1957).

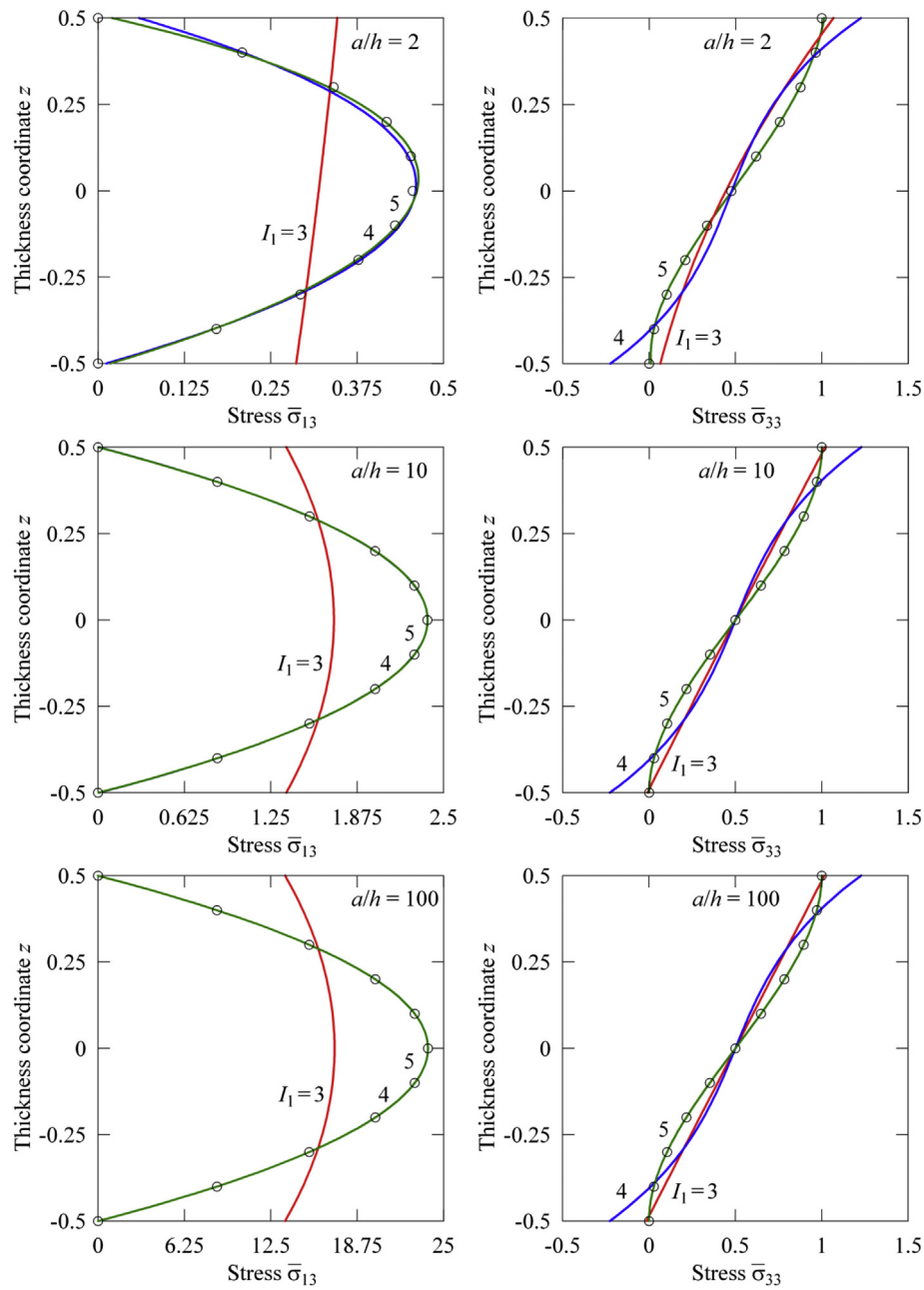

Fig. 2. Through-thickness distributions of transverse stresses for a single-layer square plate: SaS solution (—) for $I_1 = 3,4$ and 5, and Vlasov's closed form solution (○).

results of Savoia and Reddy (1995) in the case of $a/h = 4$ is presented. The difference is explained by missing the transverse thermal effects in their laminated plate formulation. As can be seen, the boundary conditions for transverse stresses and the continuity conditions for a heat flux and transverse stresses at interfaces are satisfied exactly. This statement is confirmed in Fig. 4 by means of logarithmic errors

$$\delta_i^- = \lg|\bar{\sigma}_{i3}(-0.5)|, \quad \delta_i^+ = \lg|\bar{\sigma}_{i3}(0.5)|, \tag{48}$$

which help to assess the accuracy of fulfilling the boundary conditions for transverse stresses on outer surfaces of the plate. These results show that in conventional plate theories based on the

Table 3
Results for a sandwich plate with $a/h = 4$.

I_n	$\bar{u}_1(0.5)$	$\bar{u}_2(0.5)$	$\bar{u}_3(0)$	$\bar{\sigma}_{11}(-0.5)$	$\bar{\sigma}_{22}(0.5)$	$\bar{\sigma}_{12}(0.5)$	$\bar{\sigma}_{13}(0)$	$\bar{\sigma}_{23}(0)$	$\bar{\sigma}_{33}(0.4)$	$\bar{\Theta}(-0.4)$	$\bar{q}_3(0.4)$
3	0.052456	2.5830	−2.9392	332.66	349.76	41.398	−10.939	12.040	−25.507	0.37896	9.9029
5	0.054167	2.5802	−2.9033	350.82	331.95	41.381	−11.022	11.792	0.51090	0.38012	8.9332
7	0.054168	2.5802	−2.9409	351.12	331.64	41.381	−11.022	11.793	0.17558	0.38011	8.9458
9	0.054168	2.5802	−2.9409	351.12	331.64	41.381	−11.022	11.793	0.17731	0.38011	8.9457
11	0.054168	2.5802	−2.9409	351.12	331.64	41.381	−11.022	11.793	0.17730	0.38011	8.9457

Table 4
Results for a sandwich plate with $a/h = 10$.

I_n	$\overline{u}_1(0.5)$	$\overline{u}_2(0.5)$	$\overline{u}_3(0)$	$\overline{\sigma}_{11}(-0.5)$	$\overline{\sigma}_{22}(0.5)$	$\overline{\sigma}_{12}(0.5)$	$\overline{\sigma}_{13}(0)$	$\overline{\sigma}_{23}(0)$	$\overline{\sigma}_{33}(0.4)$	$\overline{\Theta}(-0.4)$	$\overline{q}_3(0.4)$
3	0.085280	0.93377	−3.0367	356.99	376.44	16.007	−10.033	10.114	−4.9568	0.48257	24.657
5	0.085389	0.93377	−3.0377	360.41	372.94	16.009	−10.045	10.077	0.015751	0.48261	24.251
7	0.085389	0.93377	−3.0373	360.42	372.93	16.009	−10.045	10.077	0.0052274	0.48261	24.252
9	0.085389	0.93377	−3.0373	360.42	372.93	16.009	−10.045	10.077	0.0052362	0.48261	24.252
11	0.085389	0.93377	−3.0373	360.42	372.93	16.009	−10.045	10.077	0.0052362	0.48261	24.252

second, third and fourth order approximations of displacements in the thickness direction the boundary conditions for transverse stresses are never satisfied. To solve such a problem, we need to start with $I_n = 9$ for thick plates and $I_n = 6$ for moderately thick plates.

7. Analytical solution for laminated anisotropic plates in cylindrical bending

Here, we study a laminated anisotropic plate in cylindrical bending subjected to thermomechanical loading. The boundary

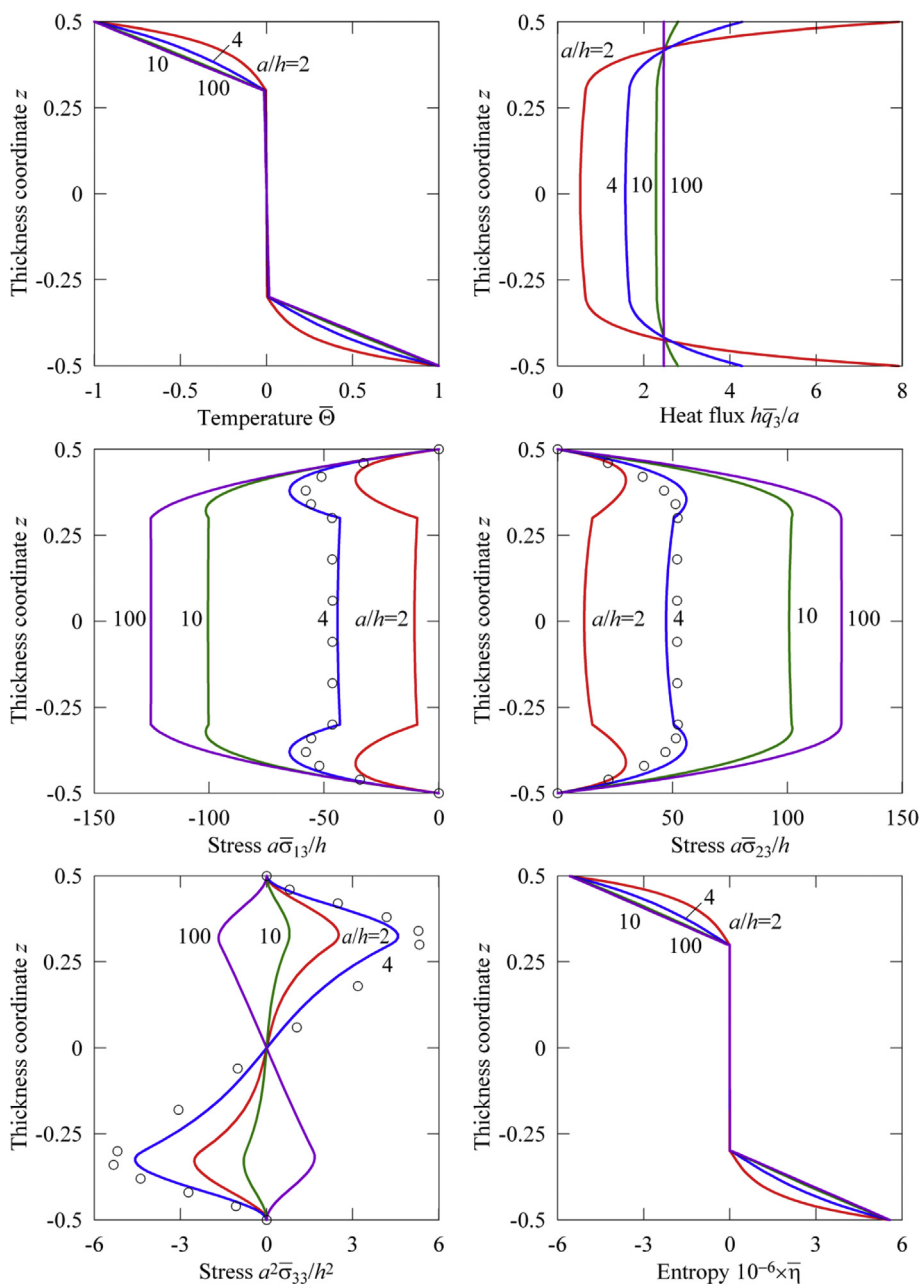

Fig. 3. Through-thickness distributions of temperature, heat flux, transverse stresses and entropy for a sandwich plate: SaS solution (—) for $I_1 = I_2 = I_3 = 11$ and Savoia and Reddy (○).

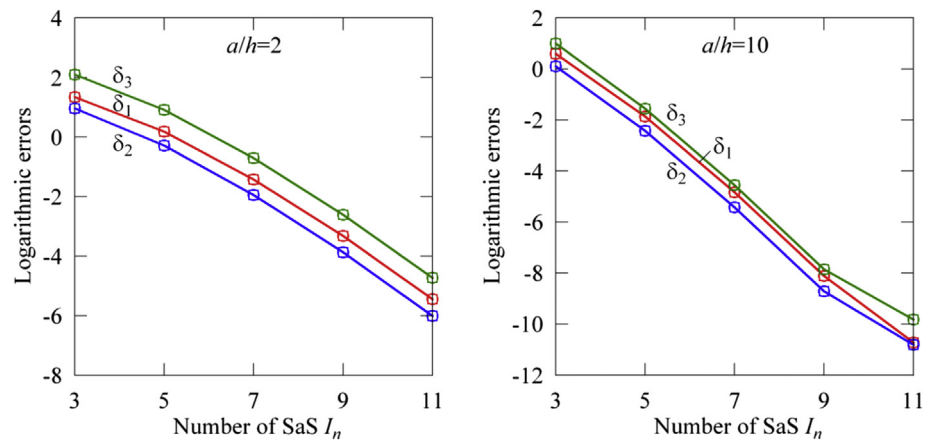

Fig. 4. Accuracy of satisfying the boundary conditions δ_i^- and δ_i^+ on bottom (○) and top (□) surfaces of the sandwich plate.

Table 5
Results for an angle-ply plate with $a/h = 5$.

I_n	$10\overline{u}_1(0.5)$	$10\overline{u}_2(0.5)$	$\overline{u}_3(0)$	$10\overline{\sigma}_{11}(-0.5)$	$100\overline{\sigma}_{13}(-0.25)$	$100\overline{\sigma}_{23}(0.25)$	$100\overline{\sigma}_{33}(0.25)$	$\overline{\Theta}(0.25)$	$\overline{q}_3(0.25)$	$\overline{\eta}(0.25)$
3	−5.7814	1.7803	1.7049	−2.1688	0.61235	−1.1563	7.8971	0.32457	−8.8888	364.07
5	−5.6540	1.7338	1.6575	−2.0507	0.98221	−1.4364	0.05346	0.32719	−7.2800	366.22
7	−5.6539	1.7338	1.6575	−2.0492	0.98142	−1.4367	0.15040	0.32714	−7.3220	366.19
9	−5.6539	1.7338	1.6575	−2.0492	0.98141	−1.4366	0.14830	0.32714	−7.3216	366.19
11	−5.6539	1.7338	1.6575	−2.0492	0.98141	−1.4366	0.14831	0.32714	−7.3215	366.19
13	−5.6539	1.7338	1.6575	−2.0492	0.98141	−1.4366	0.14831	0.32714	−7.3215	366.19
Exact	−5.654	1.734	1.657	−2.049	0.98	−1.44	0.148			

conditions for the simply supported plate with edges maintained at the reference temperature are written as

$$\sigma_{11}^{(n)} = \sigma_{12}^{(n)} = u_3^{(n)} = \Theta^{(n)} = 0 \quad \text{at } x_1 = 0 \text{ and } x_1 = a, \tag{49}$$

where a is the width of the plate. To satisfy boundary conditions, we search for the analytical solution by a method of Fourier series expansions

$$\Theta^{(n)i_n} = \sum_r \Theta_r^{(n)i_n} \sin\frac{r\pi x_1}{a}, \tag{50}$$

$$u_1^{(n)i_n} = \sum_r u_{1r}^{(n)i_n} \cos\frac{r\pi x_1}{a}, \quad u_2^{(n)i_n} = \sum_r u_{2r}^{(n)i_n} \cos\frac{r\pi x_1}{a},$$
$$u_3^{(n)i_n} = \sum_r u_{3r}^{(n)i_n} \sin\frac{r\pi x_1}{a}, \tag{51}$$

where r is the wave number along the x_1-direction. The external loads are also expanded in Fourier series.

The use of Fourier series (50) and (51) in Eqs. (9), (10), (13), (18), (22), (24), (28), (33), (37) and (38) leads to

$$J = \sum_r J_r\left(\Theta_r^{(n)i_n}\right), \tag{52}$$

$$\Pi = \sum_r \Pi_r\left(u_{ir}^{(n)i_n}, \Theta_r^{(n)i_n}\right). \tag{53}$$

Invoking variational equations (19), (52) and (26), (53), we arrive at two systems of linear algebraic equations

$$\frac{\partial J_r}{\partial \Theta_r^{(n)i_n}} = 0, \tag{54}$$

$$\frac{\partial \Pi_r}{\partial u_{ir}^{(n)i_n}} = 0 \tag{55}$$

of order K and $3K$, where $K = \sum_n I_n - N + 1$. Thus, temperatures $\Theta_r^{(n)i_n}$ and displacements $u_{ir}^{(n)i_n}$ of SaS of the nth layer can be found using a method of Gaussian elimination.

The described algorithm was performed with the Symbolic Math Toolbox, which incorporates symbolic computations into the numeric environment of MATLAB. This permits the derivation

Table 6
Results for an angle-ply plate with $a/h = 10$.

I_n	$10\overline{u}_1(0.5)$	$10\overline{u}_2(0.5)$	$\overline{u}_3(0)$	$10\overline{\sigma}_{11}(-0.5)$	$100\overline{\sigma}_{13}(-0.25)$	$100\overline{\sigma}_{23}(0.25)$	$100\overline{\sigma}_{33}(0.25)$	$\overline{\Theta}(0.25)$	$\overline{q}_3(0.25)$	$\overline{\eta}(0.25)$
3	−6.9909	1.6846	4.0149	−1.7233	0.13772	−1.0591	3.0296	0.55829	−14.078	624.76
5	−6.9647	1.6741	3.9926	−1.6606	0.34644	−1.2356	0.007521	0.55860	−13.374	624.82
7	−6.9647	1.6741	3.9926	−1.6602	0.34671	−1.2356	0.013008	0.55860	−13.379	624.83
9	−6.9647	1.6741	3.9926	−1.6602	0.34671	−1.2356	0.012955	0.55860	−13.379	624.83
11	−6.9647	1.6741	3.9926	−1.6602	0.34671	−1.2356	0.012955	0.55860	−13.379	624.83

of the analytical solutions of the SaS formulation for laminated anisotropic plates in cylindrical bending with a specified accuracy.

As a numerical example, we consider a two-layer angle-ply plate with the stacking sequence [45/−45] and ply thicknesses $h_1 = h_2 = h/2$ made of the graphite-epoxy composite. The mechanical properties of the composite are taken as follows: $E_L = E_0$, $E_T = E_0/10$, $G_{LT} = E_0/20$, $G_{TT} = E_0/50$, $\nu_{LT} = \nu_{TT} = 0.25$, $\alpha_L = \alpha_0$, $\alpha_T = 7.2\alpha_0$, $k_L = 100k_0$, $k_T = k_0$, $\rho = 1800$ kg/m^3 and $c_v = 900$ J/kgK, where $E_0 = 2 \times 10^{11}$ Pa, $\alpha_0 = 5 \times 10^{-6}$ 1/K and $k_0 = 0.5$ W/mK.

The plate is loaded on the top surface by the sinusoidally distributed temperature while the bottom surface is maintained at the reference temperature, that is

$$\Theta^{[N]} = \Theta_0 \sin\frac{\pi x_1}{a}, \quad \Theta^{[0]} = 0, \tag{56}$$

where $\Theta_0 = 1$ K and $T_0 = 293$ K. To compare the results derived with the 3D exact solution of thermoelasticity (Vel and Batra, 2001), we accept $a = 1$ m and introduce dimensionless variables as functions of the z-coordinate

$$\bar{u}_1 = u_1(a/4, z)/a\alpha_0\Theta_0, \quad \bar{u}_2 = u_2(3a/4, z)/a\alpha_0\Theta_0,$$
$$\bar{u}_3 = u_3(a/2, z)/a\alpha_0\Theta_0,$$

$$\bar{\sigma}_{11} = \sigma_{11}(a/2, z)/E_0\alpha_0\Theta_0, \quad \bar{\sigma}_{\alpha 3} = \sigma_{\alpha 3}(a/4, z)/E_0\alpha_0\Theta_0,$$
$$\bar{\sigma}_{33} = \sigma_{33}(a/2, z)/E_0\alpha_0\Theta_0,$$

$$\bar{\Theta} = \Theta(a/2, z)/\Theta_0, \quad \bar{q}_3 = aq_3(a/2, z)/k_0\Theta_0,$$
$$\eta = \eta(a/2, z)\Big/E_0\alpha_0^2\Theta_0, \quad z = x_3/h.$$

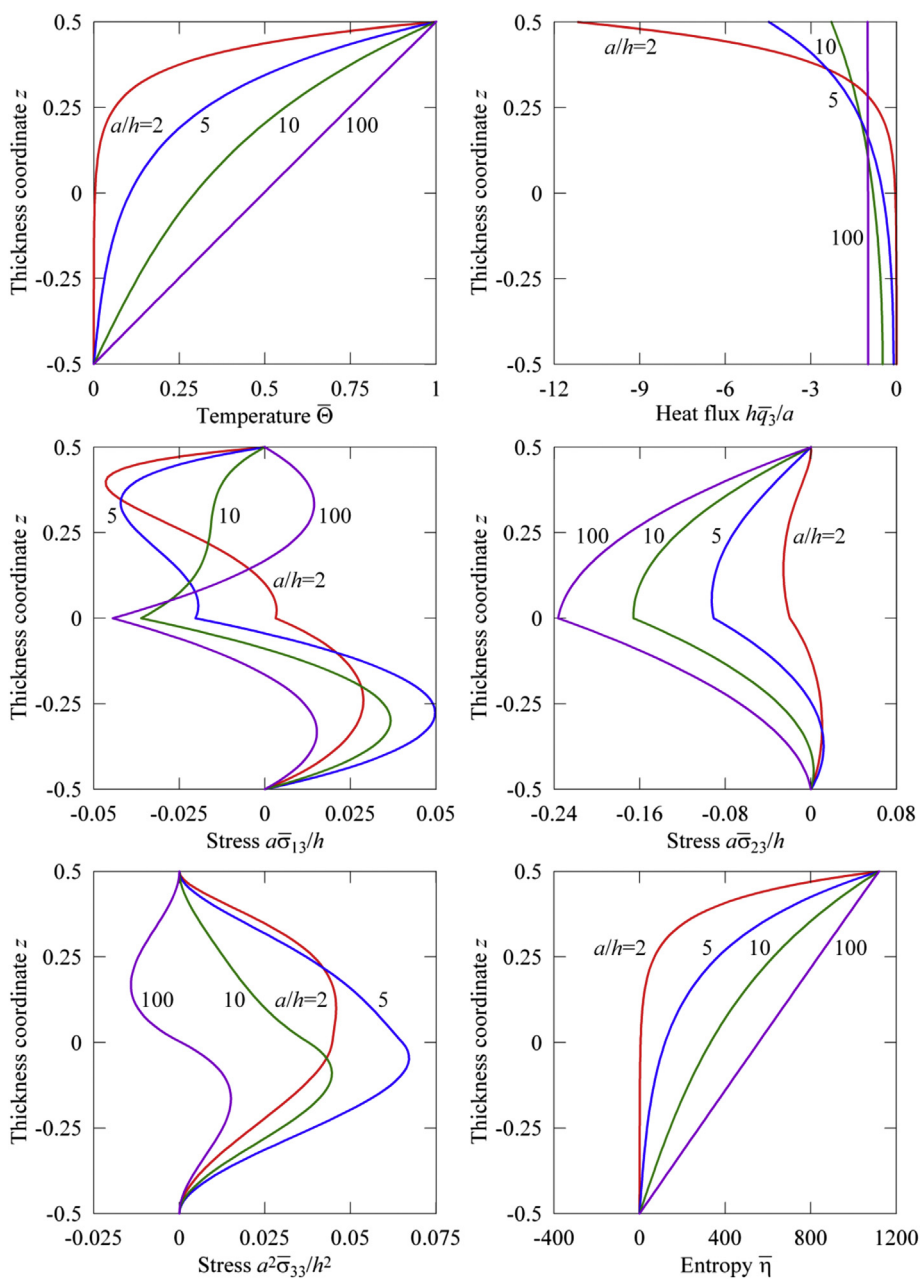

Fig. 5. Through-thickness distributions of temperature, heat flux, transverse stresses and entropy for an angle-ply plate in cylindrical bending for $l_1 = l_2 = 11$.

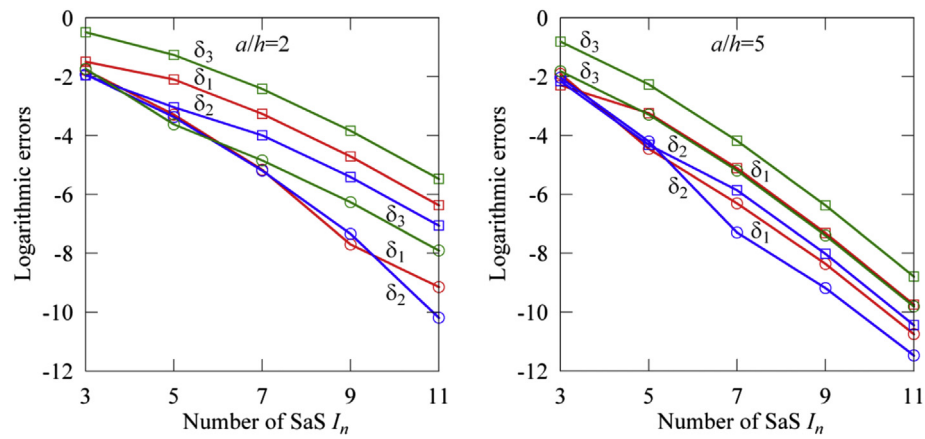

Fig. 6. Accuracy of satisfying the boundary conditions δ_i^- and δ_i^+ on bottom (○) and top (□) surfaces of the angle-ply plate.

The data listed in Tables 5 and 6 show that the SaS method permits the derivation of analytical solutions for thick angle-ply plates with a prescribed accuracy using the sufficient number of SaS. Fig. 5 presents the distributions of the temperature, heat flux, transverse stresses and entropy through the thickness of the plate for different values of the slenderness ratio a/h by choosing 11 SaS for each layer. As can be seen, the boundary conditions for transverse stresses on the outer surfaces and the continuity conditions for a heat flux and transverse stresses at the interface are satisfied again exactly. This statement is confirmed convincingly in Fig. 6 by using logarithmic errors (48), which characterize the accuracy of fulfilling the boundary conditions for transverse stresses on the bottom and top surfaces of the angle-ply plate. These results show that in conventional plate formulations utilizing second and third order approximations of displacements in the thickness direction the boundary conditions for transverse normal stresses are never satisfied. To solve such a problem, the higher order approximations are needed starting with $I_n = 7$ for thick plates and $I_n = 5$ for moderately thick plates. It is interesting to note also that the proposed SaS method provides a monotonic convergence that is impossible with *equally spaced* SaS (Kulikov and Plotnikova, 2011).

8. Analytical solution for antisymmetric angle-ply plates

Consider next a simply supported antisymmetric angle-ply rectangular plate subjected to temperature loading distributed sinusoidally on the bottom and top surfaces.

$$\Theta^{[0]} = \Theta_0 \sin\frac{r\pi x_1}{a}\sin\frac{s\pi x_2}{b}, \quad \Theta^{[N]} = -\Theta_0 \sin\frac{r\pi x_1}{a}\sin\frac{s\pi x_2}{b}. \tag{57}$$

It is well established (Noor and Burton, 1990; Savoia and Reddy, 1992, 1995) that we can search for the analytical solution of the problem as follows:

$$\Theta^{(n)i_n} = \overline{\Theta}_0^{(n)i_n} \sin\frac{r\pi x_1}{a}\sin\frac{s\pi x_2}{b} + \tilde{\Theta}_0^{(n)i_n} \cos\frac{r\pi x_1}{a}\cos\frac{s\pi x_2}{b}, \tag{58}$$

$$\begin{aligned} u_1^{(n)i_n} &= \overline{u}_{10}^{(n)i_n} \cos\frac{r\pi x_1}{a}\sin\frac{s\pi x_2}{b} + \tilde{u}_{10}^{(n)i_n} \sin\frac{r\pi x_1}{a}\cos\frac{s\pi x_2}{b}, \\ u_2^{(n)i_n} &= \overline{u}_{20}^{(n)i_n} \sin\frac{r\pi x_1}{a}\cos\frac{s\pi x_2}{b} + \tilde{u}_{20}^{(n)i_n} \cos\frac{r\pi x_1}{a}\sin\frac{s\pi x_2}{b}, \\ u_3^{(n)i_n} &= \overline{u}_{30}^{(n)i_n} \sin\frac{r\pi x_1}{a}\sin\frac{s\pi x_2}{b} + \tilde{u}_{30}^{(n)i_n} \cos\frac{r\pi x_1}{a}\cos\frac{s\pi x_2}{b}. \end{aligned} \tag{59}$$

The use of relations (58) and (59) in Eqs. (9), (10), (13), (18), (22), (24), (33), (37) and (38) leads to.

$$J = J\left(\overline{\Theta}_0^{(n)i_n}, \tilde{\Theta}_0^{(n)i_n}\right), \tag{60}$$

$$\Pi = \Pi\left(\overline{u}_{i0}^{(n)i_n}, \tilde{u}_{i0}^{(n)i_n}, \overline{\Theta}_0^{(n)i_n}, \tilde{\Theta}_0^{(n)i_n}\right). \tag{61}$$

Invoking variational equations (19), (60) and (26), (61) the following systems of linear algebraic equations of orders $2K$ and $6K$ are obtained:

$$\frac{\partial J}{\partial \overline{\Theta}_0^{(n)i_n}} = 0, \quad \frac{\partial J}{\partial \tilde{\Theta}_0^{(n)i_n}} = 0, \tag{62}$$

Table 7
Results for the unsymmetric angle-ply plate with $a/h = 4$.

I_n	$\overline{u}_1(0.5)$	$\overline{u}_3(0)$	$\overline{\sigma}_{11}(-0.5)$	$\overline{\sigma}_{12}(0.5)$	$\overline{\sigma}_{13}(0.25)$	$\tilde{\sigma}_{13}(0.25)$	$\overline{\sigma}_{33}(0.25)$	$\tilde{\sigma}_{33}(0.25)$	$\overline{\Theta}(0.25)$	$\tilde{\Theta}(0.25)$	$\overline{q}_3(0.25)$
3	2.0154	−3.5218	54.229	112.53	3.8370	22.629	46.852	35.104	−0.26185	0.23471	4.0000
5	2.2910	−4.1102	127.59	151.80	−8.0048	34.303	8.7527	14.509	−0.30086	0.24531	2.2963
7	2.2949	−4.1179	132.69	152.24	−6.9499	33.219	3.2107	8.9775	−0.30022	0.24674	2.5068
9	2.2949	−4.1179	133.01	152.23	−7.0044	33.273	3.5188	9.2855	−0.30025	0.24670	2.4935
11	2.2949	−4.1179	133.02	152.23	−7.0028	33.272	3.5090	9.2757	−0.30025	0.24671	2.4939
13	2.2949	−4.1179	133.02	152.23	−7.0028	33.272	3.5092	9.2759	−0.30025	0.24671	2.4939

Table 8
Results for the unsymmetric angle-ply plate with $a/h = 10$.

I_n	$\bar{u}_1(0.5)$	$\bar{u}_3(0)$	$\bar{\sigma}_{11}(-0.5)$	$\bar{\sigma}_{12}(0.5)$	$\bar{\sigma}_{13}(0.25)$	$\tilde{\sigma}_{13}(0.25)$	$\bar{\sigma}_{33}(0.25)$	$\tilde{\sigma}_{33}(0.25)$	$\bar{\Theta}(0.25)$	$\tilde{\Theta}(0.25)$	$\bar{q}_3(0.25)$
3	1.5132	−8.6313	118.13	160.54	1.5982	13.358	18.017	15.449	−0.40974	0.15819	10.000
5	1.5709	−8.9944	141.82	170.57	−5.3058	20.934	1.3139	2.6692	−0.41234	0.16073	8.9303
7	1.5710	−8.9945	142.23	170.56	−5.1795	20.807	0.86386	2.2198	−0.41233	0.16075	8.9569
9	1.5710	−8.9945	142.23	170.56	−5.1806	20.808	0.86837	2.2243	−0.41233	0.16075	8.9566
11	1.5710	−8.9945	142.23	170.56	−5.1806	20.808	0.86835	2.2243	−0.41233	0.16075	8.9566

$$\frac{\partial \Pi}{\partial \bar{u}_{i0}^{(n)i_n}} = 0, \quad \frac{\partial \Pi}{\partial \tilde{u}_{i0}^{(n)i_n}} = 0, \tag{63}$$

where $K = \sum_n I_n - N + 1$. The linear systems (62) and (63) are solved independently by using a method of Gaussian elimination. As accepted in this paper, the described algorithm was performed with the Symbolic Math Toolbox of MATLAB.

As a numerical example, we study an antisymmetric two-ply square plate [45/−45] composed of the graphite-epoxy composite with material properties given in section 6.2. The plate with geometrical parameters $h_1 = h_2 = h/2$ and $a = b = 1$ m is subjected to temperature loading (57) with $r = s = 1$, $\Theta_0 = 1$ K and $T_0 = 293$ K. For numerical calculations it is convenient to introduce the following dimensionless variables at crucial points as functions of the z-coordinate:

$$\bar{u}_1 = u_1(0, a/2, z)/a\alpha_r\Theta_0, \quad \bar{u}_3 = u_3(a/2, a/2, z)/a\alpha_r\Theta_0,$$
$$\bar{\sigma}_{11} = \sigma_{11}(a/2, a/2, z)/E_r\alpha_r\Theta_0,$$

$$\bar{\sigma}_{12} = \sigma_{12}(0, 0, z)/E_r\alpha_r\Theta_0, \quad \bar{\sigma}_{13} = \sigma_{13}(0, a/2, z)/E_r\alpha_r\Theta_0,$$
$$\tilde{\sigma}_{13} = \sigma_{13}(a/2, 0, z)/E_r\alpha_r\Theta_0,$$

$$\bar{\sigma}_{33} = \sigma_{33}(a/2, a/2, z)/E_r\alpha_r\Theta_0, \quad \tilde{\sigma}_{33} = \sigma_{33}(0, 0, z)/E_r\alpha_r\Theta_0,$$
$$\bar{\eta} = \eta(a/2, a/2, z)\Big/E_r\alpha_r^2\Theta_0,$$

$$\bar{\Theta} = \Theta(a/2, a/2, z)/\Theta_0, \quad \tilde{\Theta} = \Theta(0, 0, z)/\Theta_0,$$
$$\bar{q}_3 = aq_3(a/2, a/2, z)/k_r\Theta_0,$$

where $E_r = 1$ GPa, $\alpha_r = 10^{-6}$ 1/K, $k_r = 1$ W/mK and $z = x_3/h$.

Tables 7 and 8 demonstrate again the high potential of the proposed laminated plate formulation based on the SaS method since it can be applied efficiently to derivation of analytical

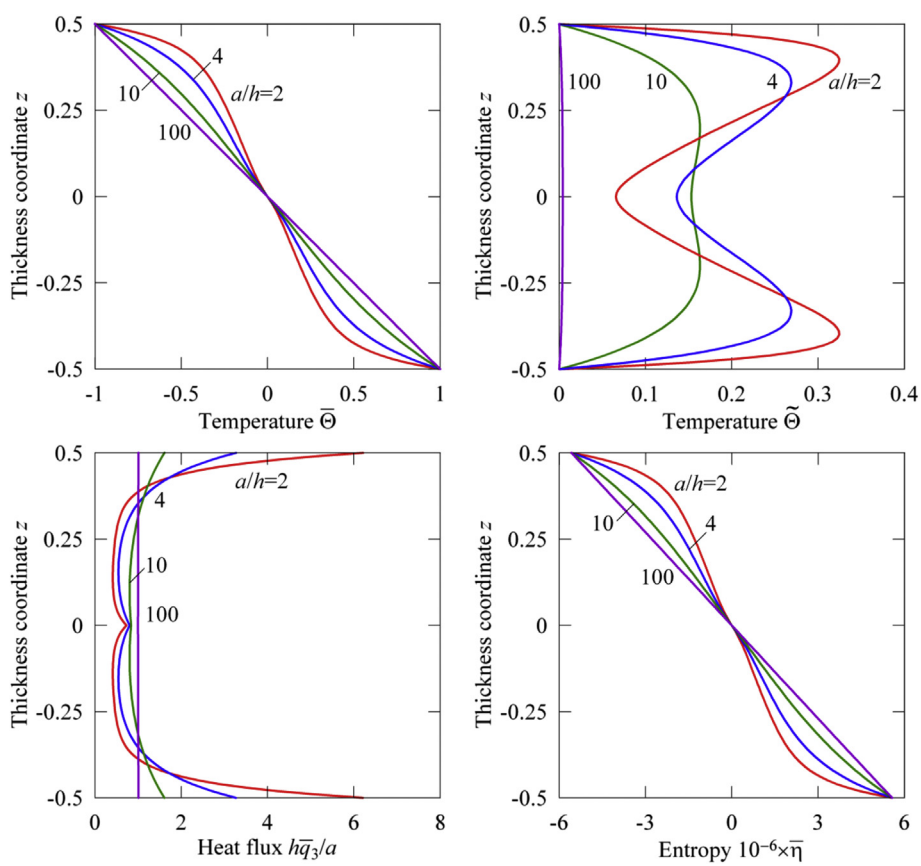

Fig. 7. Through-thickness distributions of temperature, heat flux and entropy for the unsymmetric angle-ply plate for $I_1 = I_2 = 11$.

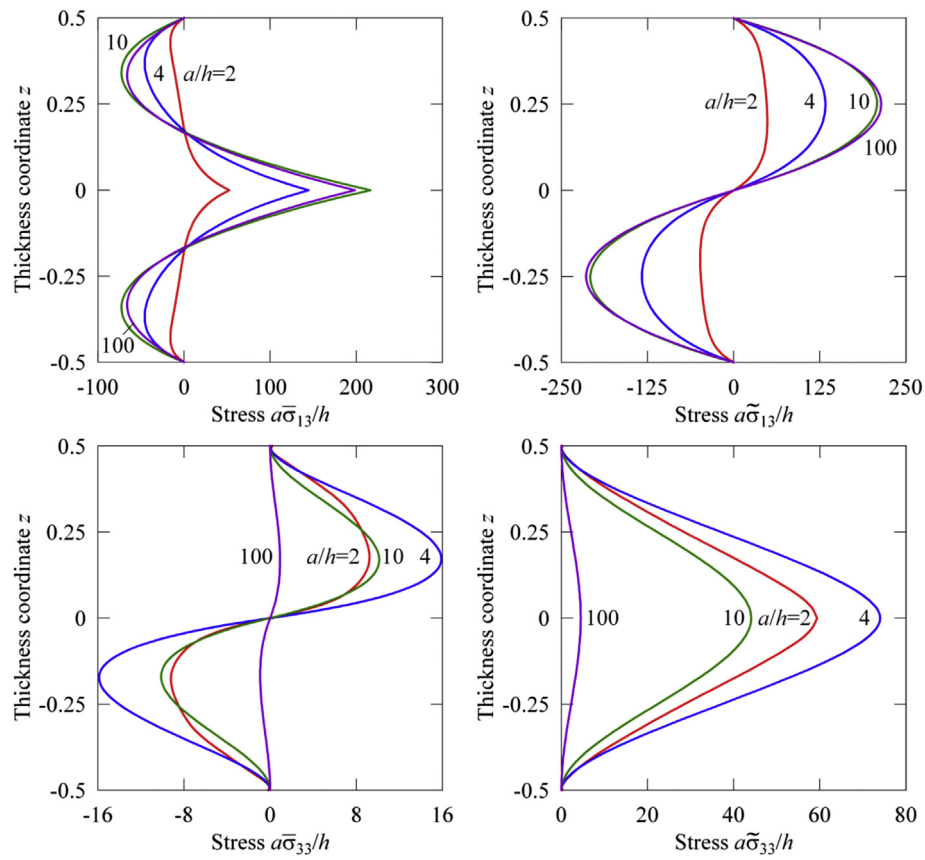

Fig. 8. Through-thickness distributions of transverse stresses for the unsymmetric angle-ply plate for $l_1 = l_2 = 11$.

solutions for unsymmetric angle-ply plates with a prescribed accuracy employing the sufficiently large number of SaS. Figs. 7 and 8 display distributions of temperature, heat flux, entropy and transverse stresses in the thickness direction for different slenderness ratios using eleven SaS for each layer. As can be seen, the boundary conditions for transverse stresses on the bottom and top surfaces and the continuity conditions for a heat flux and transverse stresses at the interface are satisfied correctly.

9. Conclusions

An efficient method of solving the steady-state problems of 3D thermoelasticity for laminated orthotropic and anisotropic plates has been proposed. It is based on a new method of SaS located at Chebyshev polynomial nodes inside the layers. This allows one to minimize uniformly the error due to Lagrange interpolation. The thermal stress analysis of laminated plates is based on the 3D constitutive equations and gives an opportunity to obtain the analytical solutions for thick and thin cross-ply and angle-ply plates with a prescribed accuracy.

Acknowledgment

This work was supported by Russian Ministry of Education and Science under Grant No 9.137.2014/K and by Russian Foundation for Basic Research under Grant No 13-01-00155.

Appendix

Figs. A1–A3 list the implementation of the numerical algorithm developed in section 6.1 by means of three MATLAB modules. The first module serves for the computation of Lagrange polynomials (8), their derivatives (11) and integrals of Lagrange polynomials (25). The second module provides the calculation of displacements and strains of sampling surfaces (13) and (18). The third one serves for computing the total potential energy (33) and solving the linear algebraic equation (45). This implementation emphasizes readability of the MATLAB code and could be recommended to the reader for his/her more general implementations.

```
% Number of Sampling Surfaces In
% Calculation of Transverse Coordinates of Sampling Surfaces
for i=1:In
  theta_three(In-i+1)=cos(pi*(2*i-1)/2/In)*h/2;
end
% Calculation of Lagrange Polynomials
for i=1:In
  for j=1:In
    if(i~=j)
      L(i)=L(i)*(theta3-theta_three(j))/(theta_three(i)-theta_three(j));
    end
  end
end
% Calculation of Derivatives of Lagrange Polynomials
for i=1:In
  M(i)=diff(L(i),theta3);
end
% Calculation of Integrals from Lagrange Polynomials
for i=1:In
  for j=1:In
    Lambda(i,j)=double(int(L(i)*L(j),theta3,-h/2,h/2));
  end
end
```

Fig. A1. MATLAB module for calculating Lagrange polynomials, derivatives and integrals.

```
% Calculation of Loads
p3plus=p0*sin(pi*theta1/a)*sin(pi*theta2/b);
% Calculation of Displacements of Sampling Surfaces
for i=1:In
   u1(i)=U(i)*cos(pi*theta1/a)*sin(pi*theta2/b);
   u2(i)=U(In+i)*sin(pi*theta1/a)*cos(pi*theta2/b);
   u3(i)=U(2*In+i)*sin(pi*theta1/a)*sin(pi*theta2/b);
end
% Calculation of Strains of Sampling Surfaces
for i=1:In
  beta1(i)=sym('0');
  beta2(i)=sym('0');
  beta3(i)=sym('0');
end
for i=1:In
  for j=1:In
    beta1(i)=beta1(i)+subs(M(j),theta_three(i))*u1(j);
    beta2(i)=beta2(i)+subs(M(j),theta_three(i))*u2(j);
    beta3(i)=beta3(i)+subs(M(j),theta_three(i))*u3(j);
  end
end
for i=1:In
  epsilon11(i)=diff(u1(i),theta1);
  epsilon22(i)=diff(u2(i),theta2);
  epsilon33(i)=beta3(i);
  epsilon12(i)=(diff(u1(i),theta2)+diff(u2(i),theta1))/2;
  epsilon13(i)=(beta1(i)+diff(u3(i),theta1))/2;
  epsilon23(i)=(beta2(i)+diff(u3(i),theta2))/2;
end
```

Fig. A2. MATLAB module for calculating displacements and strains of sampling surfaces.

```
% Calculation of Total Potential Energy
% Stress Resultants H11(i), H22(i), H33(i), H12(i), H13(i), H23(i)
Energy=sym('0');
for i=1:In
  Energy=Energy+H11(i)*epsilon11(i)/2+H22(i)*epsilon22(i)/2+H33(i)*epsilon33(i)/2;
  Energy=Energy+H12(i)*epsilon12(i)+H13(i)*epsilon13(i)+H23(i)*epsilon23(i);
end
for i=1:In
  Energy=Energy-p3plus*u3(i)*subs(L(i),theta3,h/2);
end
First_Integral=int(Energy,theta1,0,double(a));
PE=int(First_Integral,theta2,0,double(b));
PE=vpa(PE,32);
% Solution of System of Linear Equations
for i=1:In
  Der(i)=diff(PE,u10(i));
  Der(In+i)=diff(PE,u20(i));
  Der(2*In+i)=diff(PE,u30(i));
end
Res=solve(Der);
```

Fig. A3. MATLAB module for calculating a total potential energy and solving linear algebraic equations.

References

Bhaskar, K., Varadan, T.K., Ali, J.S.M., 1996. Thermoelastic solutions for orthotropic and anisotropic composite laminates. Compos. Part B Eng. 27, 415–420.

Burden, R.L., Faires, J.D., 2010. Numerical Analysis, ninth ed. Brooks/Cole, Cengage Learning, Boston.

Carrera, E., 2000. An assessment of mixed and classical theories for the thermal stress analysis of orthotropic multilayered plates. J. Therm. Stress. 23, 797–831.

Carrera, E., 2005. Transverse normal strain effect on thermal stress analysis of homogeneous and layered plates. AIAA J. 43, 2232–2242.

Carrera, E., Ciuffreda, A., 2004. Closed form solutions to assess multilayered plate theories for various thermal stress problems. J. Therm. Stress. 27, 1001–1031.

Cheng, Z.Q., Batra, R.C., 2000. Three-dimensional thermoelastic deformations of a functionally graded elliptic plate. Compos. Part B Eng. 31, 97–106.

Kashtalyan, M., 2004. Three-dimensional elasticity solution for bending of functionally graded rectangular plates. Eur. J. Mech. A/Solids 23, 853–864.

Kulikov, G.M., 2001. Refined global approximation theory of multilayered plates and shells. J. Eng. Mech. 127, 119–125.

Kulikov, G.M., Carrera, E., 2008. Finite deformation higher-order shell models and rigid-body motions. Int. J. Solids Struct. 45, 3153–3172.

Kulikov, G.M., Plotnikova, S.V., 2011. Solution of statics problems for a three-dimensional elastic shell. Dokl. Phys. 56, 448–451.

Kulikov, G.M., Plotnikova, S.V., 2012a. Exact 3D stress analysis of laminated composite plates by sampling surfaces method. Compos. Struct. 94, 3654–3663.

Kulikov, G.M., Plotnikova, S.V., 2012b. On the use of sampling surfaces method for solution of 3D elasticity problems for thick shells. ZAMM – J. Appl. Math. Mech. 92, 910–920.

Kulikov, G.M., Plotnikova, S.V., 2013. Advanced formulation for laminated composite shells: 3D stress analysis and rigid-body motions. Compos. Struct. 95, 236–246.

Kulikov, G.M., Plotnikova, S.V., 2014. Heat conduction analysis of laminated shells by a sampling surfaces method. Mech. Res. Commun. 55, 59–65.

Murakami, H., 1993. Assessment of plate theories for treating the thermomechanical response of layered plates. Compos. Eng. 3, 137–149.

Noor, A.K., Burton, W.S., 1990. Three-dimensional solutions for antisymmetrically laminated anisotropic plates. J. Appl. Mech. 57, 182–188.

Noor, A.K., Kim, Y.H., Peters, J.M., 1994. Transverse shear stresses and their sensitivity coefficients in multilayered composite panels. AIAA J. 32, 1259–1269.

Pagano, N.J., 1969. Exact solutions for composite laminates in cylindrical bending. J. Compos. Mater. 3, 398–411.

Pagano, N.J., 1970a. Exact solutions for rectangular bidirectional composites and sandwich plates. J. Compos. Mater. 4, 20–34.

Pagano, N.J., 1970b. Influence of shear coupling in cylindrical bending of anisotropic laminates. J. Compos. Mater. 4, 330–343.

Reddy, J.N., 2004. Mechanics of Laminated Composite Plates and Shells: Theory and Analysis, second ed. CRC Press, Boca Raton.

Reddy, J.N., Cheng, Z.Q., 2001. Three-dimensional thermomechanical deformations of functionally graded rectangular plates. Eur. J. Mech. A/Solids 20, 841–855.

Robaldo, A., Carrera, E., Benjeddou, A., 2005. Unified formulation for finite element thermoelastic analysis of multilayered anisotropic composite plates. J. Therm. Stress. 28, 1031–1065.

Robaldo, A., Carrera, E., 2007. Mixed finite elements for thermoelastic analysis of multilayered anisotropic plates. J. Therm. Stress. 30, 165–194.

Savoia, M., Reddy, J.N., 1992. A variational approach to three-dimensional elasticity solutions of laminated composite plates. J. Appl. Mech. 59, S166–S175.

Savoia, M., Reddy, J.N., 1995. Three-dimensional thermal analysis of laminated composite plates. Int. J. Solids Struct. 32, 593–608.

Srinivas, S., Rao, A.K., 1970. Bending, vibration and buckling of simply supported thick orthotropic rectangular plates and laminates. Int. J. Solids Struct. 6, 1463–1481.

Tauchert, T.R., 1980. Thermoelastic analysis of laminated orthotropic slabs. J. Therm. Stress. 3, 117–132.

Tungikar, V.B., Rao, K.M., 1994. Three dimensional exact solution of thermal stresses in rectangular composite laminate. Compos. Struct. 27, 419–430.

Vel, S.S., Batra, R.C., 2001. Generalized plane strain thermoelastic deformation of laminated anisotropic thick plates. Int. J. Solids Struct. 38, 1395–1414.

Vel, S.S., Batra, R.C., 2002. Exact solution for thermoelastic deformations of functionally graded thick rectangular plates. AIAA J. 40, 1421–1433.

Vlasov, B.F., 1957. On the Bending of Rectangular Thick Plate. In: Vestnik Moskovskogo Universiteta. Matematika, Mekhanika, Astronomia, vol. 2, pp. 25–31.

Woodward, B., Kashtalyan, M., 2011. Three-dimensional elasticity solution for bending of transversely isotropic functionally graded plates. Eur. J. Mech. A/Solids 30, 705–718.